Earth's Future

RESEARCH ARTICLE
10.1029/2018EF001119

Projecting Changes in Expected Annual Damages From Riverine Flooding in the United States

C. Wobus[1], P. Zheng[2], J. Stein[2], C. Lay[2], H. Mahoney[2], M. Lorie[3], D. Mills[2], R. Spies[1], B. Szafranski[1], and J. Martinich[4]

[1]Lynker Technologies, Boulder, CO, USA, [2]Abt Associates, Boulder, CO, USA, [3]Corona Environmental Consulting, Louisville, CO, USA, [4]U.S. Environmental Protection Agency, Washington, DC, USA

Key Points:
- We used multifrequency flood maps to quantify expected annual damages from inland flooding at 376 locations across the United States
- Expected annual damages estimated from floods of multiple magnitudes are typically 5–7 times higher than damages estimated from regulatory "100-year" floods alone
- Projected damages more than double under 3 degrees Celsius of warming for most regions, underscoring the importance of limiting future temperature changes

Supporting Information:
- Supporting Information S1
- Data Set S1

Correspondence to:
C. Wobus,
cwobus@lynkertech.com

Citation:
Wobus, C., Zheng, P., Stein, J., Lay, C., Mahoney, H., Lorie, M., et al. (2019). Projecting changes in expected annual damages from riverine flooding in the United States. *Earth's Future*, *7*, 516–527. https://doi.org/10.1029/2018EF001119

Received 3 DEC 2018
Accepted 27 MAR 2019
Accepted article online 8 APR 2019
Published online 3 MAY 2019

Abstract Inland flood risk in the United States is most often conveyed through maps of 1% annual exceedance probability (AEP) or "100-year" floodplains. However, monetary damages from flooding arise from a full distribution of events, including floods both larger and smaller than the 1% AEP event. Furthermore, floodplains are not static, since both the frequency and magnitude of flooding are likely to change in a warming climate. We explored the implications of a changing frequency and magnitude of flooding across a wide spectrum of flood events, using a sample of 376 watersheds in the United States where floodplains from multiple recurrence intervals have been mapped. Using an inventory of assets within these mapped floodplains, we first calculated expected annual damages (EADs) from flooding in each watershed under baseline climate conditions. We find that the EAD is typically a factor of 5–7 higher than the expected damages from 100-year events alone and that much of these damages are attributable to floods smaller than the 1% AEP event. The EAD from flooding typically increases by 25–50% under a 1 °C warming scenario and in most regions more than double under a 3 °C warming scenario. Further increases in EAD are not as pronounced beyond 3 °C warming, suggesting that most of the projected increases in flood damages will have already occurred, for most regions of the country, by that time. Adaptations that protect against today's 100-year flood will have increasing benefits in a warmer climate by also protecting against more frequent, smaller events.

1. Introduction

Floods are among the most damaging natural disasters in the world, causing tens of billions of dollars in monetary damages globally each year (e.g., Pielke & Downton, 2000; Smith & Matthews, 2015). Because a warmer atmosphere can hold more moisture than a cooler atmosphere (e.g., O'Gorman & Muller, 2010), climate change is expected to change the frequency and magnitude of flooding, and therefore flood damages, worldwide (e.g., Dottori et al., 2018; Willner et al., 2018). Multiple extreme floods in the United States over recent years have refocused attention on the role of climate change in exacerbating damages from both inland and coastal flooding (e.g., Trenberth et al., 2018; van der Wiel et al., 2017). A number of recent studies have also estimated future changes in flood risk and damages both globally (e.g., Alfieri et al., 2017; Jongman et al., 2014; Knighton et al., 2017; Ward et al., 2017) and within the United States(e.g., AECOM, 2013; Wobus et al., 2017). Many of these studies indicate that inland flood damages are increasing and are projected to continue increasing, in a warmer world.

In the United States, most of the available data to inform inland flooding risk and damage are focused on the "100-year" flood or the flood that has a 1% chance of occurring in any given year (e.g., AECOM, 2013; Wobus et al., 2017). This focus on the 1% annual exceedance probability (AEP) flood is largely a result of the National Flood Insurance Program (NFIP), which requires that homeowners with federally backed mortgages purchase flood insurance if their property lies within the 1% AEP floodplain. The 1% AEP floodplains are thus more comprehensively mapped across much of the United States than floodplains with other exceedance probabilities. However, the expected annual damages (EADs) from inland flooding stem not only from 1% AEP events but from a full distribution of potential flood events whose depths and associated damages vary with recurrence interval (RI; Arnell, 1989). Larger, less frequent floods can be expected to cause more damage than a 1% AEP event when they occur, whereas smaller events can be expected to cause less damage but occur more frequently.

Because the EAD from flooding stems from the full area under a flood damage-probability curve, the degree to which flood damages will change in a warmer world will depend on both the amount of damage caused by each individual event and on the relative change in the frequency of events with different magnitudes. Recent work has estimated the potential changes in floods of different magnitudes globally (e.g., Alfieri et al., 2017; Kettner et al., 2018), and changes across the full distribution of flood events have been linked to future damages in specific regions around the world (e.g., Dottori et al., 2018; Hattermann et al., 2014). However, to date we have not found a study focused on linking changes in the frequency of floods of multiple magnitudes in the United States to the changes in damages that those floods are expected to cause.

In this study, we combine data from multifrequency flood mapping projects available across the United States (Federal Emergency Management Agency, FEMA, 2010) with a flood damage tool developed for the U.S. Army Corps of Engineers (e.g., Wobus et al., 2017) to estimate the EADs from flood events in 376 HUC10 watersheds distributed primarily across the eastern United States (HUC10 is a unit of watershed measure as part of a nested classification system of U.S. watersheds; there are approximately 22,000 watersheds at this scale in the United States; see Seaber et al., 1987). The multifrequency flood mapping products come from FEMA's Risk mapping, assessment, and planning (RiskMAP) program, which uses standard hydraulics methods to generate maps of expected water surface elevations for RIs ranging from the 2-year through 500-year flood event (FEMA, 2018). Using these data to represent a baseline level of flood risk, we then estimate changes in the frequency of floods at each of these historical RIs, under future scenarios corresponding to temperature increases ranging from 1 to 5 °C above an historical baseline for the contiguous United States (CONUS). Using this approach, we estimate the changes in EADs from flooding in each location where multifrequency flood hazard data are available.

Finally, we estimate the benefits of adaptations to protect against inland flooding. Although there have been several studies predicting the beneficial impacts of adaptation to coastal flood risk (e.g., Dinan, 2017; Hinkel et al., 2014; Neumann et al., 2015), research into adaption to future riverine flood risk is more limited. Ward et al. (2017) developed and tested a framework for predicting future costs and benefits of adaptation, concluding that levees may be cost beneficial in many urban areas. Other studies have focused on smaller regions or evaluating specific options for individual locations (e.g., Aerts et al., 2014; Kirshen et al., 2012). Using the multifrequency flood mapping data available through the RiskMAP program, we evaluate the benefits of adaptations to protect against the 1% AEP event. While the adaptation model we utilize is simple, it provides a first-order view of how the benefits of flood protection investments might change across the range of climate change scenarios we examined.

2. Methods

2.1. Data Collection and Synthesis

We obtained data from the 118 available RiskMAP databases for the nation, from the FEMA Flood Map Service Center at the FEMA website (https://msc.fema.gov/portal/home). We organized all of the available floodplain data into HUC10 watersheds, which we used as our minimum spatial unit for analysis. The final data set included 275 HUC10 watersheds with floodplain maps for five RIs (10, 25, 50, 100, and 500 years) and an additional 101 HUC10s with maps for three RIs (10, 100, and 500 years).

The details of our analysis are described in supporting information S1; a brief summary follows here. First, to tabulate the assets within each mapped floodplain, we overlaid the floodplain maps with census block data summarizing the total property assets per block and land cover data to estimate the distribution of those assets within the census blocks. We then calculated the damages resulting from a flood of each RI by following the methods described in Wobus et al. (2017): Specifically, we intersected the floodplain depth grids with the developed portion of each census block, as determined from a three-way intersection of flood depth, census block, and developed land use types from the national land cover database. Once the three-way intersection was complete, we used the flood depth grids to develop a probability distribution of flood depths for each floodplain-census block intersection.

Using these flood depth distributions, we calculated monetary damage for the developed portion of each census block-floodplain intersection by first extracting the total dollar value of built assets from FEMA's

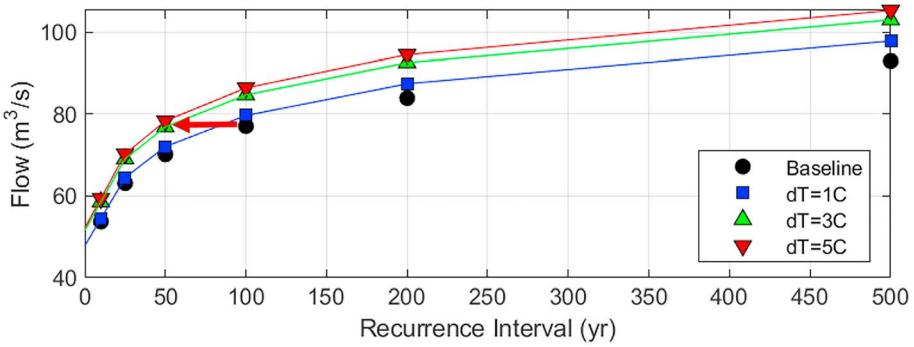

Figure 1. Example of projected changes in flow as a function of temperature, for a location at the outlet of a single HUC10 watershed. Changes in the future recurrence interval for 10-, 25-, 50-, 100-, and 500-year events were calculated by matching each of the baseline flow magnitudes to their future recurrence intervals, as shown schematically by the red arrow relating the baseline 100-year event to the 50-year event at dT = 3 °C.

HAZUS-MH General Building Stock inventory (FEMA, 2015). The General Building Stock inventory provides estimates of the number and aggregate dollar value of multiple types of residential, commercial, and industrial buildings for each census block in the United States. We assumed a homogeneous distribution of each building type within the developed portion of each census block-floodplain intersection. We then used depth-damage functions published by the U.S. Army Corps of Engineers (2000) for each category of buildings in the HAZUS-MH inventory to calculate the percentage loss for each building type within that census block. This process was combined with the total value of each building type within the developed portion of each census block-floodplain intersection to calculate the damages resulting from each flood RI. Once we compiled the damages for each census block-floodplain intersection, we aggregated these damages up to the HUC10 level for further analysis.

2.2. Calculating EADs

We used the asset inventory and RIs from the flood maps to calculate the EAD from flooding by first combining the estimated damages from each RI (calculated as described in section 2.1) with its probability of occurrence. Using these raw data, we developed a damage-probability curve for each HUC10. We then calculated the EADs for each HUC10 as the area under this damage-probability curve (e.g., Arnell, 1989). It is important to note that while the HUC10 was the minimum mapping unit used for our analysis, there are portions of each HUC10 where no floodplain maps are available. Thus, while our results provide a measure of the expected damages from flooding in different watersheds, these cost estimates are likely to underestimate the total flood risk in each watershed.

For this study, we assumed that no damages accrue for events smaller than the baseline 10-year event. Since we did not have data on the spatial extent of floodplains larger than the 500-year event, we also did not extrapolate damages for events larger than the 500-year event. Thus, the EADs reported here are those resulting from events ranging from the historical 10- through 500-year flood events.

2.3. Climate Change Analysis

For the hydrologic analysis, we utilized downscaled hydrology projections developed by a consortium of federal agencies including the U.S. Army Corps of Engineers, the U.S. Bureau of Reclamation, and other federal agencies, which includes daily flow projections from 29 different global climate models (GCMs) downscaled using the bias correction and spatial disaggregation method (e.g., Reclamation, 2014; Wobus et al., 2017). At each of the nodes corresponding to the downstream limit of the HUC10s with RiskMAP data, we extracted annual maximum flow time series from 20-year windows corresponding to a baseline period (2001–2020) and from future periods corresponding to CONUS-average temperature changes of 1, 2, 3, 4, and 5 °C above the baseline period for each GCM. For example, CanESM2 reaches a 3 °C threshold above baseline in the year 2065 (Table S1); for this model, the outputs from 2056 to 2075 were used to represent a 3 °C temperature increase. Because not all 29 of the GCMs reach a CONUS-average temperature threshold of 5 °C by the end of the century, we based our analysis on just the 14

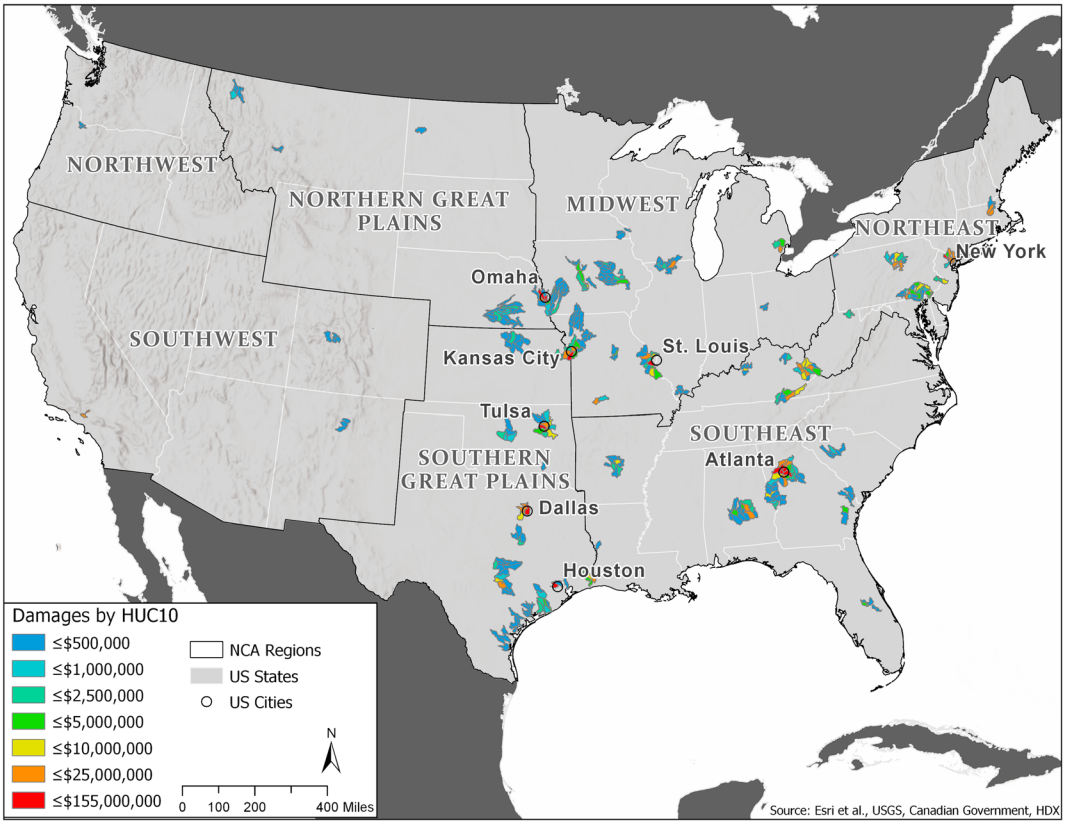

Figure 2. Map of expected annual damage nationwide, based on all HUC10s with at least three recurrence intervals mapped. All values are in 2014 dollars. National climate assessment (NCA) regions are labeled in capital letters.

models that reach this threshold by 2100. Thus, each temperature threshold is represented by a sample of 280 annual flow maxima (14 models × 20 years), which we used to estimate the parameters of a generalized extreme value (GEV) distribution. Supporting information S2 summarizes the models used in the analysis, as well as the effect of calculating future flow statistics using just these 14 models, compared to using the full set of 29 models used by Wobus et al. (2017).

Table 1
Summary of All HUC10 Watersheds With EAD Exceeding $25 Million in the Baseline Period, Based on Calculations Using Three Recurrence Intervals for Each RiskMAP Study

U.S. metro region	EAD (Three RIs)	HUC10	NCA region
Houston	$154,459,049	1204010403	Southern Great Plains
Atlanta NE	$72,025,017	0313000112	Southeast
Omaha	$60,513,187	1023000602	Northern Great Plains
St. Louis	$49,621,749	0714010210	Midwest
Kansas City E	$45,794,685	1030010101	Southern Great Plains
Tulsa	$40,301,532	1111010103	Southern Great Plains
Atlanta NE	$38,298,553	0313000111	Southeast
Atlanta SE	$33,154,394	0307010301	Southeast
NYC suburbs	$33,138,121	0203010305	Northeast
Dallas	$31,208,539	1203010501	Southern Great Plains
Atlanta SW	$29,151,968	0313000202	Southeast
Atlanta SW	$26,419,002	0313000201	Southeast
Omaha	$25,453,375	1023000606	Midwest

Note. EAD = expected annual damage; RI = recurrence interval.

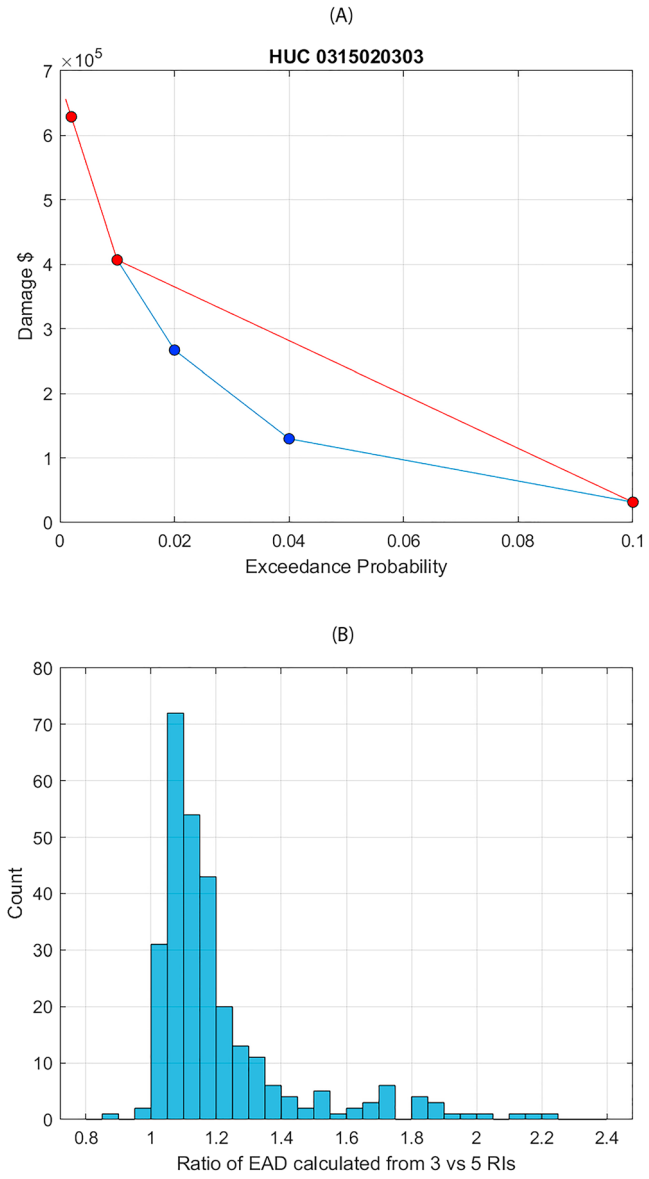

Figure 3. Effect on expected annual damage of using three recurrence intervals (RIs) versus five RIs to calculate the area under the damage curve. (a) Example of added damages resulting from a damage-probability curve constrained by only three recurrence intervals (red curve) versus five (blue curve): Note that the area under the curve is larger for the curve that is unconstrained by the 2% and 4% annual exceedance probability events. (b) Ratio of expected annual damage calculated from three versus five return intervals, for the 276 sites with all five return intervals mapped. EAD = expected annual damage.

Using the GEV parameters estimated for the baseline period, we calculated the magnitude of flow corresponding to each of the events mapped in the RiskMAP studies (e.g., the "10-year" or 10% AEP through "500-year" or 0.2% AEP events). Because our approach relies on a delta method (i.e., we look at model to model changes in flow and superimpose those changes on observations), it is not critical that the modeled flows perfectly replicate observations. However, as shown in Wobus et al. (2017), the multiscale parameter regionalization approach used to develop the simulated flows provides a reasonable representation of flows at this scale. Using these baseline flow magnitudes and the GEV parameters for each of the future temperature thresholds, we then calculated the AEP for each of the baseline events in the RiskMAP studies under each warming scenario. These future exceedance probabilities were calculated by matching the baseline flow magnitudes for the 10-,25-,50-,100-, and 500-year events to their future RIs, which were linearly interpolated between each calculated value (Figure 1). Thus, for each temperature threshold we estimate the future frequency of occurrence of each event mapped in the RiskMAP studies. We linked these changes in frequency to the damage estimates for each mapped event to calculate the change in EADs within each HUC10.

2.4. Incorporating Adaptation

In order to include the mitigating effects of flood protection into our analysis, we also asked the simple question of how investments in adaptation today will perform in the future. To answer this question, we assumed that today's investments are designed to protect against the current 1% AEP event. This is a reasonable assumption given the incentives created by the NFIP (e.g., Kousky, 2016). For each RiskMAP study location, we thus assumed that investments today will prevent future damages from all floods with magnitudes smaller than today's 1% AEP event ("avoided damages"). We assumed that damages for floods larger (i.e., lower probability) than today's 1% AEP event will still be incurred ("residual damages"). Using this simple rule, we can examine trends in future avoided and residual damages under the full range of future climate scenarios. Importantly, the installation and maintenance costs of these protective adaptations are not quantified in this study, resulting in an overestimate of the net economic benefits. This is an important area for future research (e.g., Ward et al., 2017).

3. Results

3.1. Baseline EADs

For the 376 HUC10s with all three RIs mapped, the EADs from flooding range from nearly zero damage in areas with relatively low population density, to as much as $50–150 million in watersheds that include population centers like Houston, St. Louis, Atlanta, and Omaha. Figure 2 shows the baseline EAD by HUC10 watershed, with national climate assessment regions labeled for reference. Table 1 lists all of the HUC10 watersheds with EADs exceeding $25 million in the baseline period, along with the major population centers contained in each of those watersheds.

Note that based on our methodology, the EAD is determined in part by the number of RIs mapped in each location. In particular, with only three RIs the EAD will typically be overestimated relative to the EAD calculated from five RIs, simply because there are fewer data points to constrain the shape of the damage-probability curve (Figure 3a). Although we used the larger data set for our analysis (e.g., the 376 HUC10s

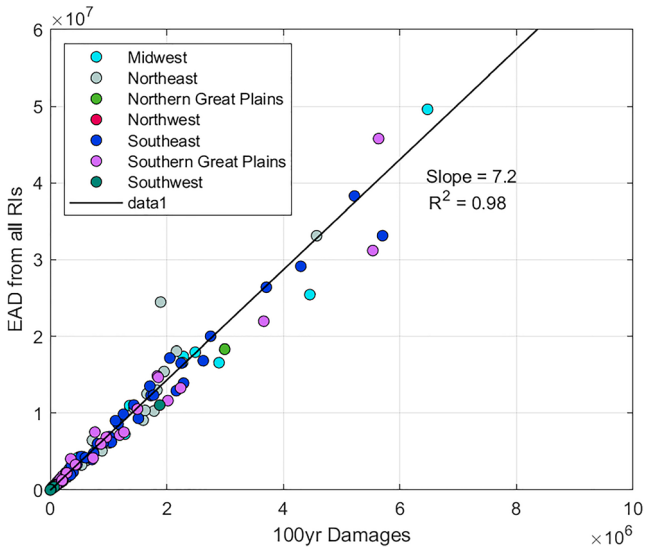

Figure 4. Comparison between expected annual damage (EAD) from all return intervals and "expected damages" from 100-year events alone (e.g., 1% of 100-year damages) for all sites with three recurrence intervals mapped. Colors of dots correspond to national climate assessment regions shown in Figure 1.

with three RIs mapped), we also wanted to understand the degree to which the EAD might be overestimated by using this data set. We compared the EAD based on three RIs to the EAD based on five RIs, for the 275 locations where all five RIs were mapped. In the majority of cases, the degree to which EAD is overestimated when based on only three RIs is between approximately 10% and 30% (Figure 3b). Thus, the actual EAD estimates described herein are likely to be biased 10–30% high compared to what we might have estimated if we had all five RIs mapped at all locations. However, since the RiskMAP data set with only three RIs is substantially more extensive than the data set with five RIs, we report all results based on estimates from three RIs.

Nationwide, there is also a much larger sample of floodplains where only the 100-year floodplain is mapped than there is for the more comprehensive RiskMAP studies. Thus it is also useful to evaluate the correlation between the EADs calculated herein and the damages expected from 100-year events alone (e.g., Wobus et al., 2017), as this ratio could be used to support a first-order approximation of national-scale EAD from inland flooding (see supporting information S3). As shown in Figure 4, there is a strong correlation between the EAD from all RIs and the expected damages from just 100-year events. This is to be expected because locations with dense development within 100-year floodplains are also likely to have dense development within floodplains with other RIs, whereas locations in more rural areas are more likely to have limited development throughout their high-risk areas. While the relationship between total EAD and expected damages from 100-year events alone varies slightly by region, the EAD calculated from all events is typically between 5 and 7 times higher than the expected damages from 100-year events alone, assuming that damaged areas are restored to baseline following each flood event.

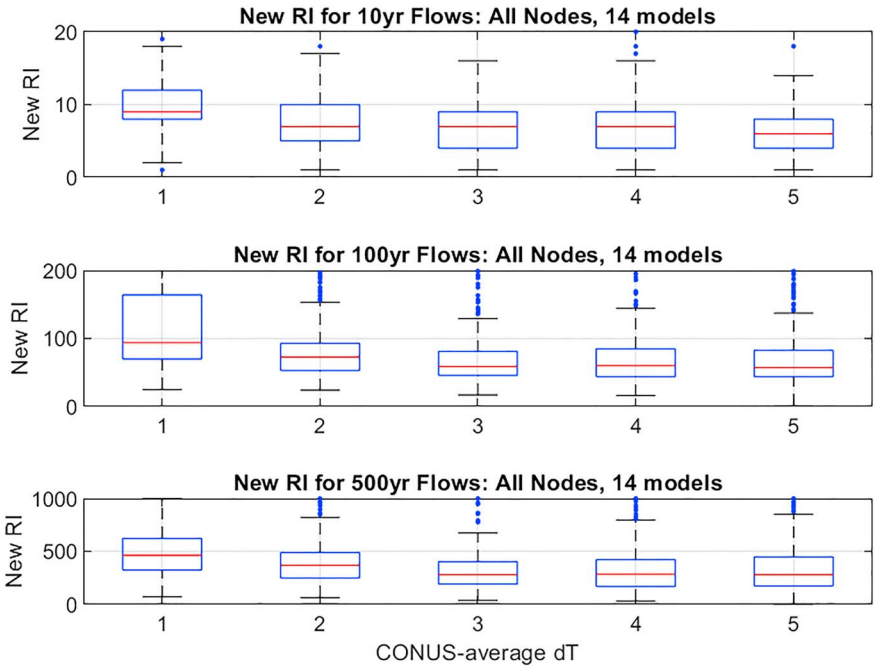

Figure 5. Projected future recurrence intervals (RIs) for events with historical magnitudes corresponding to (a) 10-, (b) 100-, and (c) 500-year events. Note that the majority of change in future recurrence intervals occurs between 1 and 3 °C above historical baseline. CONUS = contiguous United States.

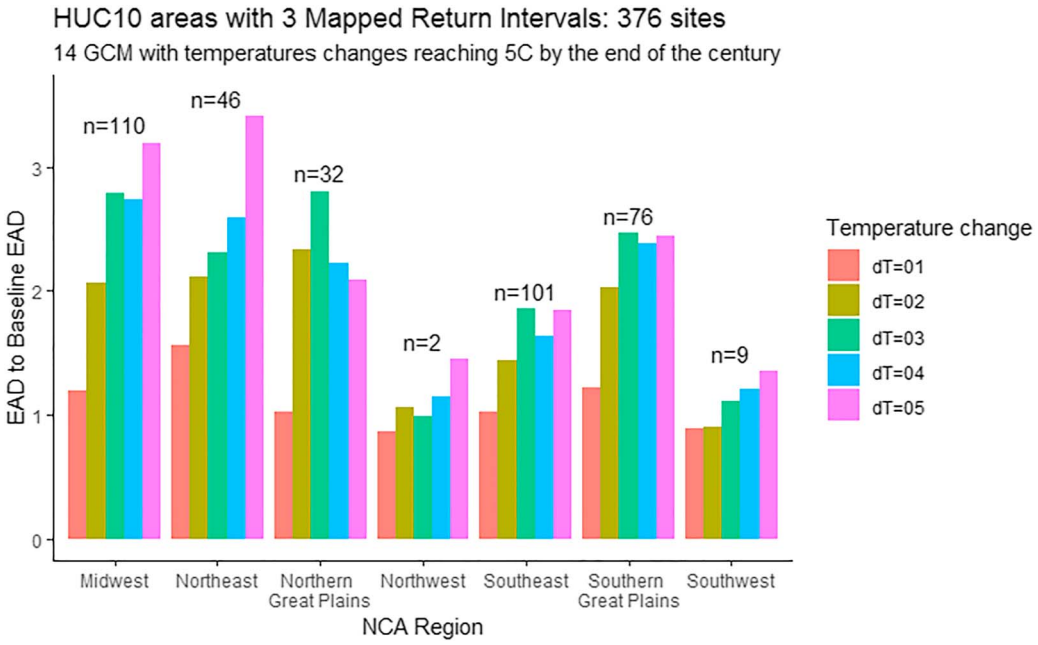

Figure 6. Changes in EAD as a function of temperature change above baseline, compiled for each of the NCA regions with RiskMAP data. *N* values above each bar plot indicate the number of HUC10s with RiskMAP data in each region. GCM = global climate model; EAD = expected annual damage; NCA = national climate assessment.

3.2. Projected Effects of Climate Change

In general, each incremental increase in CONUS-average temperature results in an increase in the magnitude and frequency of floods across all return intervals. As shown in Figure 5, the majority of the change in flow frequencies occurs between d*T* values of 1 and 3 °C. For example, at a CONUS-averaged d*T* value of 1 °C, the median future return interval for a 10-year event remains approximately 10 years, whereas at 3 °C the median future return interval for this event is approximately 6 years (Figure 5a). Beyond a d*T* value of 3 °C, the median return interval for a historical 10-year event remains relatively unchanged. This pattern is similar for 100- and 500-year events (Figures 5b and 5c): The frequency of both of these events approximately doubles between a CONUS-averaged dT of 1 and 3 °C and then remains approximately steady for higher CONUS-average temperature thresholds above 3 °C. However, there are generally more outliers for these longer RIs, reflecting the higher uncertainty in the projected change in low-probability events.

When we propagate projected changes in hydrology through the calculation of changes in EAD, we find a similar result: The EADs from flooding within each region of the United States increase rapidly between temperature thresholds of 1 and 3 °C, but further increases in EAD are smaller for CONUS-averaged temperature changes of 4–5 °C (Figure 6). Changes in EADs are also unequally distributed across different regions of the United States: For example, EAD nearly triples relative to baseline between temperature thresholds of 1 and 3 °C for the Midwest and Northern Great Plains, whereas in the Southeast for the same change in temperature, EAD increases by less than a factor of 2. Projections for the Northwest and Southwest suggest smaller increases in EAD in these regions, although the limited RiskMAP studies completed in these regions make it difficult to generalize these results.

The source of increase in EAD varies slightly from region to region, but in general, the data indicate that much of the change in EAD arises from increases in the frequency of relatively small events. Figure 7 shows examples from four of the HUC10s with the largest baseline EAD nationwide: HUC 1204010403, which flows through the Houston suburbs; HUC 0714010210, which includes parts of suburban St. Louis; HUC 0203010308, which includes some of the New Jersey suburbs of New York City; and HUC 0409000302 in Southeast Michigan near Detroit. In all cases, the historical 10% AEP (10-year) event is projected to more than triple in frequency, and in some cases the frequency of the historical 10% event increases by an order

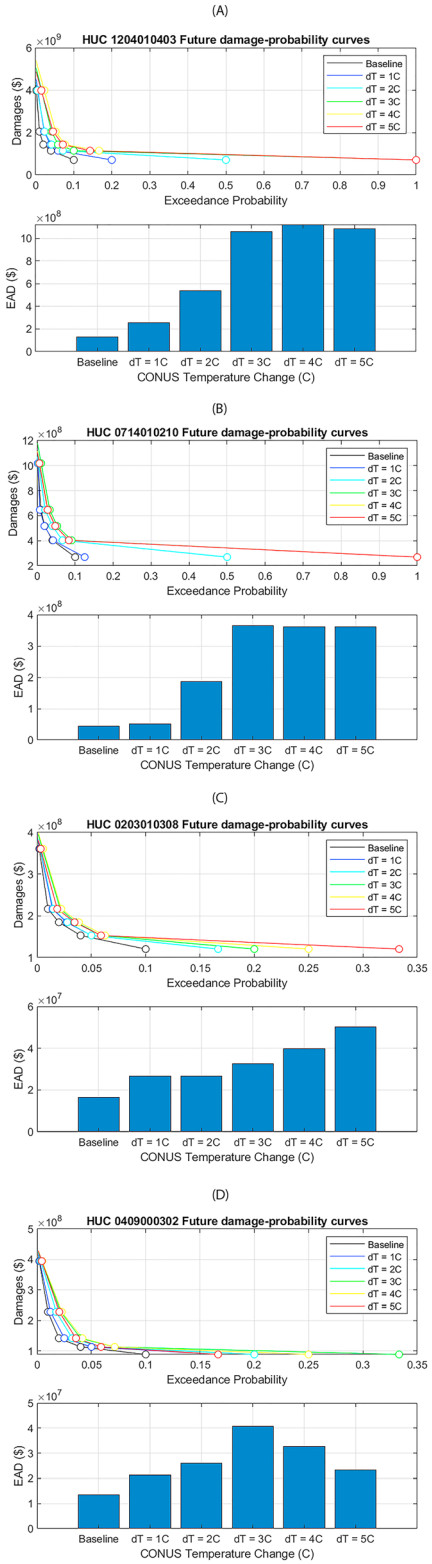

Figure 7. Changes in expected annual damages due to changes in floods of all recurrence intervals for HUC10 watersheds that include parts of the suburbs of (a) Houston, (b) St. Louis, (c) New York, and (d) Detroit. Note that for both the Houston and St. Louis HUCs, the historical 10-year event becomes approximately 5 times as frequent at 3 °C and becomes a once-per-year event at a temperature of 5 °C above baseline. EAD = expected annual damage; CONUS = contiguous United States.

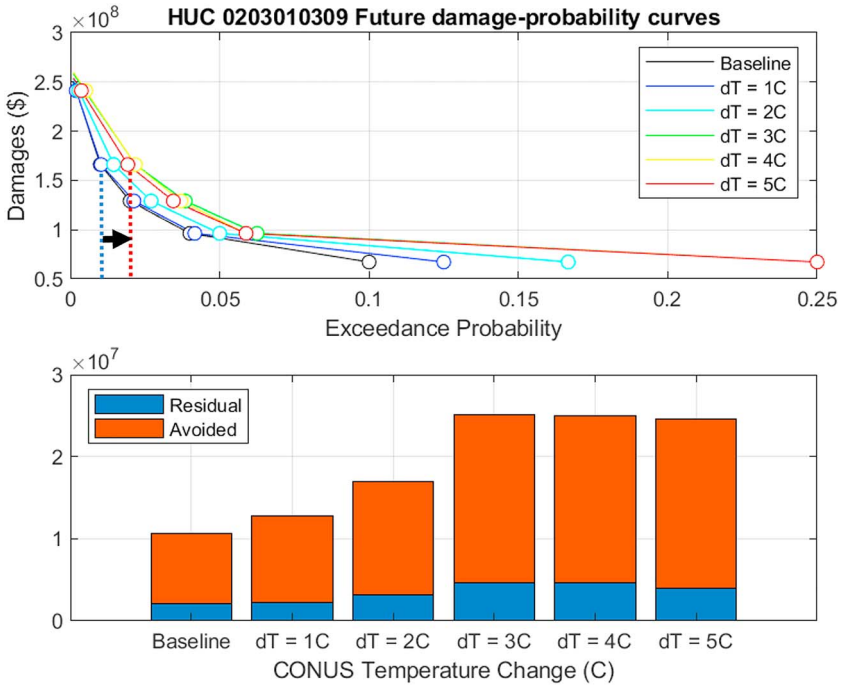

Figure 8. Example of future avoided and residual EAD assuming a community undertakes public works to protect against the baseline 1% annual exceedance probability event. A) Damage-probability curves as in Figure 7, with dashed line representing a hypothetical adaptation to the baseline 1% annual exceedance probability event (protecting against an event that would cause approximately $170 M of damage, and avoiding damage from all events smaller than this). B) With increasing temperatures, damages avoided represent an increasing fraction of the EAD, even as total EAD increases. CONUS = contiguous United States; EAD = expected annual damage.

of magnitude (e.g., the 10% AEP event becomes an annual event). For comparison, in the two examples with a tenfold increase in the frequency of the 10% AEP event, the 1% AEP event increases in frequency by only a factor of 2–3 (see Figures 7a and 7b).

3.3. The Benefits of Adaptation

All of the results summarized above use the mapped floodplains available from RiskMAP studies, which incorporate existing on-the-ground adaptation measures such as accredited levees, but assume that no further adaptation occurs to protect communities from flooding events. As described in section 2.4, we also evaluated the benefits of adaptation by assuming that communities immediately undertake further measures to protect against the baseline 1% AEP flood event. With this assumption, we can then separate the area under the damage-probability curve into two segments: The area under the curve to the right of the baseline 1% AEP event (whose probability typically increases with increasing temperature) represents the flood damages avoided from those adaptation measures, and the area under the curve to the left of the 1% AEP event represents residual damages that will occur even with protection against smaller events.

Figure 8 shows an example of how such a simple adaptation rule influences projected flooding outcomes, for a HUC10 watershed in the New York City suburbs. In this case, the 1% AEP event (shown by the dashed blue line in Figure 8a) becomes approximately 50% more frequent at a 2 °C temperature threshold, and approximately 2.5 times more frequent at a 5 °C temperature threshold (shown by the rightward shift of the dots corresponding to the 1% AEP damage value). The adaptations taken to protect against the baseline 1% AEP event will protect against all events smaller than this in the future. In this case, even though the residual damages increase through time (as shown by the area to the left of the vertical dashed line), the avoided damages increase more rapidly because the 10% AEP event becomes substantially more frequent. As a result, even though total EAD increases, the ratio of damages avoided to

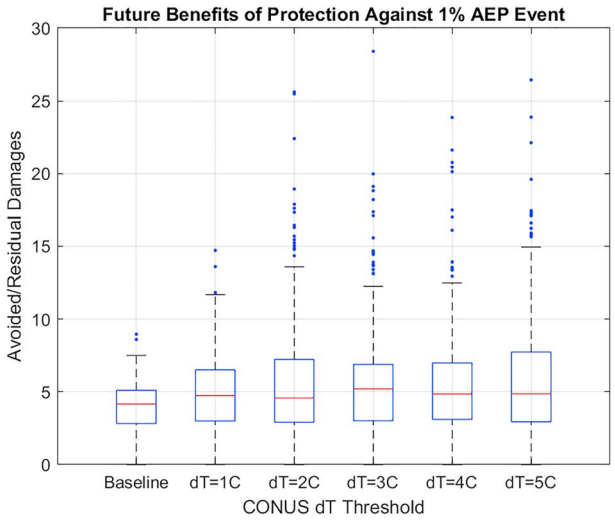

Figure 9. Ratio of avoided to residual damages for all sites with RiskMAP data, assuming protection against the baseline 1% AEP event.
AEP = annual exceedance probability; CONUS = contiguous United States.

residual damages increases through time, as shown by the progressively larger red fraction of the EAD bars in Figure 8b.

Assuming that measures are implemented to protect against today's 1% AEP event at all sites with RiskMap data, the ratio of avoided to residual damages tends to increase with each successive increase in CONUS-average temperature. For example, across all of the sites in our data set, the median ratio of avoided to residual damages in the baseline is approximately 4, whereas at a temperature threshold of 3 °C, this ratio increases to approximately 5 (Figure 9). The full distribution of avoided/residual damage ratios also shifts upward with each successive temperature increase, indicating that a larger share of EADs is projected to come from events smaller than the baseline 1% AEP events as temperatures warm. Thus, while in most cases both residual and avoided damages are projected to increase with increasing temperatures (e.g., Figure 8b), the available data indicate that today's flood protection investments will become increasingly beneficial in the future. However, to the extent that regulations continue to focus on the historical 1% AEP event, it is important to note that a larger share of future flooding will in general include events larger than the current regulatory floodplain. Scaling flood defenses with consideration of the current and future EAD across all flood magnitudes could improve the net benefits of future flood protection investments.

4. Discussion and Conclusions

Inland floods are extremely costly natural disasters, whose impacts are likely to increase in a warming climate. While the NFIP tends to focus both financial and engineering solutions on the 1% AEP event (which also protects against smaller events), we have shown here that a full spectrum of flood events contributes substantially to the EADs from flooding. Furthermore, we find that projected hydrologic impacts of climate change will also influence this full spectrum of inland flood magnitudes, which will compound future losses in the absence of both global greenhouse gas mitigation and protective adaptation measures. To optimize flood protection under a changing climate, the cost and size of flood protection investments should be weighed against both the current and future EAD across all flood magnitudes, rather than just the 1% AEP event.

While our results underscore the importance primarily of smaller events in driving EADs from flooding, our analysis also indicates that the benefits of today's adaptation investments will increase as CONUS-average temperatures rise. For example, assuming that adaptations continue to be focused on the 1% AEP event (as is currently incentivized by the NFIP), these investments are projected to protect against an increasing frequency of smaller damaging events as temperatures warm. Although data limitations do not allow us to quantify changes in residual damages due to increasing magnitudes of the most extreme floods, it is likely that the relative benefits of today's adaptations will continue to increase with rising temperatures.

All of our hydrologic projections are based on GCM outputs from the CMIP5 model ensemble (Taylor et al., 2012). CMIP5 is the most comprehensive climate model archive available, and these models have been shown to generally follow the 7% increase in extreme precipitation per degree C suggested by first principles (e.g., Trenberth, 1999; Pendergrass et al., 2015). Because our flood change projections follow a delta approach, wherein we compare model hindcasts to forecasts, we therefore expect that the underlying signal from the GCMs produces a robust projection of future change. However, all of the GCMs in this archive remain limited in their ability to resolve tropical and extratropical storms that drive large-scale flooding in some regions. GCMs also do not simulate the smaller-scale convective storms that can lead to localized flooding in some locations. To the extent that tropical and convective storms are projected to become more severe in a warming climate (e.g., Emanuel, 2013; Trenberth et al., 2018), our results will underestimate future increases in damages due to inland flooding, particularly in regions where these events dominate hydrologic extremes. In addition, the routed hydrology we used was derived from statistical downscaling,

which requires an assumption that the underlying spatial patterns in precipitation variability remain consistent as temperatures rise.

Our results also rely on the simplifying assumption that buildings are evenly distributed within the developed portions of each census block. This simplifying assumption was required in order to obtain the necessary data to implement our methodology at a national scale. Future work focused on community-level adaptation decisions could employ the methodology described here with parcel-level data on individual building values, in order to complete a full cost–benefit analysis of flood protection or building relocation investments.

Although our results clearly illustrate the benefits of flood protection, the funds available for these investments are limited. The illustrative adaptation scenario considered here of comprehensively protecting against the 1% AEP flood event would entail extremely high infrastructure, planning, and maintenance costs that are not estimated in this analysis. A more detailed analysis could model prioritization of future adaptation investments as a function of avoided damages and socioeconomic factors (e.g., income), but such an analysis is beyond the scope of this study. In addition, this analysis does not account for changes in population and development within flood risk zones. Future demographic changes could either increase or decrease damages from flooding in the future, but without reasonable means of predicting future floodplain development or policies governing development, we held these factors constant.

Finally, our analysis is necessarily limited to the parts of the country where RiskMAP studies have been conducted, and multifrequency flood mapping products are available. Notably, there is little coverage from these RiskMAP studies in the western half of the United States, making it challenging to quantitatively extrapolate our results to the national scale. Nonetheless, in the locations where we have sufficient data, our analysis suggests that most of the increase in the frequency of flood events, and associated damages, will have occurred by the time a CONUS-averaged temperature threshold of 3 °C is reached. This result underscores the urgency of limiting further increases in global temperatures: If temperatures reach a CONUS-averaged dT of 3 °C above baseline, most of the projected increases in flood damages will have already occurred, for most regions of the country. Flood damages are therefore much more sensitive to preventing more modest temperature changes (e.g., 1 or 2 °C) such that efforts to reduce anthropogenic warming will have the most significant monetary benefits if enacted quickly.

Acknowledgments
This research was funded by the U.S. Environmental Protection Agency under contract EPBPA16H0003. URLs for accessing each of the data sets used in this analysis, as well as analysis steps, are described in the supporting information. We thank Andy Wood, Naoki Mizukami, and Ethan Gutmann at the National Center for Atmospheric Research for providing routed flow data for the CONUS. We also thank two anonymous reviewers for their thorough and constructive reviews, which greatly improved the quality of this manuscript. The views expressed in this document are those of the authors and do not necessarily reflect those of their affiliated institutions.

References

AECOM (2013). The impact of climate change and population growth on the National Flood Insurance Program through 2100. Retrieved from http://www.adaptationclearinghouse.org/resources/the-impact-of-climate-change-and-population-growth-on-the-national-flood-insurance-program-through-2100.html

Aerts, J. C. J. H., Botzen, W. J. W., Emanuel, K., Lin, N., de Moel, H., & Michel-Kerjan, E. O. (2014). Evaluating flood resilience strategies for coastal megacities. *Science*, *344*(6183), 473–475. https://doi.org/10.1126/science.1248222

Alfieri, L., Bisselink, B., Dottori, F., Naumann, G., de Roo, A., Salamon, P., et al. (2017). Global projections of river flood risk in a warmer world. *Earth's Future*, *5*(2), 171–182. https://doi.org/10.1002/2016EF000485

Arnell, N. W. (1989). Expected annual damages and uncertainties in flood frequency estimation. *Journal of Water Resources Planning and Management*, *115*(1), 94–107. https://doi.org/10.1061/(ASCE)0733-9496(1989)115:1(94)

Dinan, T. (2017). Projected increases in hurricane damage in the United States: The role of climate change and coastal development. *Ecological Economics*, *138*, 186–198. https://doi.org/10.1016/j.ecolecon.2017.03.034

Dottori, F., Szewczyk, W., Ciscar, J.-C., Zhao, F., Alfieri, L., Hirabayashi, Y., et al. (2018). Increased human and economic losses from river flooding with anthropogenic warming. *Nature Climate Change*, *8*(September), 781–786. https://doi.org/10.1038/s41558-018-0257-z

Emanuel, K. A. (2013). Downscaling CMIP5 climate models shows increased tropical cyclone activity over the 21st century. *Proceedings of the National Academy of Sciences*, *110*(30), 12219–12224. https://doi.org/10.1073/pnas.1301293110

Federal Emergency Management Agency (2010). FEMA's risk mapping, assessment, and planning (Risk MAP). Retrieved from https://www.fema.gov/media-library-data/20130726–1743–25045-0785/rm_digitalelev_plan.pdf

Federal Emergency Management Agency (2015). *HAZUS-MH 2.2, FEMA's software program for multi-hazard loss estimation for potential losses from disaster*. Washington, D.C: Federal Emergency Management Agency.

Federal Emergency Management Agency (2018). Guidance for flood risk analysis and mapping, Base Level Engineering Analyses and Mapping, Guidance Document 99. Retrieved from https://www.fema.gov/media-library-data/1526489690918-2862bece100f28564-c4167aaf4b2378b/Base_Level_Engineering_Guidance_Feb_2018.pdf

Hattermann, F. F., Huang, S., Burghoff, O., Willems, W., Österle, H., Büchner, M., & Kundzewicz, Z. (2014). Modelling flood damages under climate change conditions—A case study for Germany. *Natural Hazards and Earth System Science*, *14*(12), 3151–3168. https://doi.org/10.5194/nhess-14-3151-2014

Hinkel, J., Lincke, D., Vafeidis, A. T., Perrette, M., Nicholls, R. J., Tol, R. S. J., et al. (2014). Coastal flood damage and adaptation costs under 21st century sea-level rise. *Proceedings of the National Academy of Sciences*, *111*(9), 3292–3297. https://doi.org/10.1073/pnas.1222469111

Jongman, B., Hochrainer-Stigler, S., Feyen, L., Aerts, J. C. J. H., Mechler, R., Botzen, W. J. W., et al. (2014). Increasing stress on disaster-risk finance due to large floods. *Nature Climate Change*, *4*(4), 264–268. https://doi.org/10.1038/nclimate2124

Kettner, A. J., Cohen, S., Overeem, I., Fekete, B. M., Brakenridge, G. R., & Syvitski, J. P. (2018). *Estimating Change in Flooding for the 21st Century Under a Conservative RCP Forcing: A Global Hydrological Modeling Assessment. Global Flood Hazard: Applications in Modeling, Mapping, and Forecasting* (pp. 157–167).

Kirshen, P., Merrill, S., Slovinsky, P., & Richardson, N. (2012). Simplified method for scenario-based risk assessment adaptation planning in the coastal zone. *Climatic Change*, *113*(3–4), 919–931. https://doi.org/10.1007/s10584-011-0379-z

Knighton, J., Steinschneider, S., & Walter, M. T. (2017). A vulnerability-based,bottom-up assessment of future riverine flood risk using a modified peaks-over-threshold approach and a physically based hydrologic model. *Water Resources Research*, *53*, 10043–10064. https://doi.org/10.1002/2017WR021036

Kousky, C. (2016). Disasters as learning experiences or disasters as policy opportunities? Examining Flood Insurance Purchases after Hurricanes. *Risk Analysis*, *37*(3), 517–530. https://doi.org/10.1111/risa.12646

Neumann, J. E., Emanuel, K., Ravela, S., Ludwig, L., Kirshen, P., Bosma, K., & Martinich, J. (2015). Joint effects of storm surge and sea-level rise on US Coasts: New economic estimates of impacts, adaptation, and benefits of mitigation policy. *Climatic Change*, *129*(1–2), 337–349. https://doi.org/10.1007/s10584-014-1304-z

O'Gorman, P. A., & Muller, C. J. (2010). How closely do changes in surface and column water vapor follow Clausius–Clapeyron scaling in climate change simulations?*Environmental Research Letters*, *5*(2), 025207). https://doi.org/10.1088/1748-9326/5/2/025207

Pendergrass, A. G., Lehner, F., Sanderson, B. M., & Xu, Y. (2015). Does extreme precipitation intensity depend on the emissions scenario? *Geophysical Research Letters*, *42*, 8767–8774. https://doi.org/10.1002/2015GL065854

Pielke, J., & Downton, M. W. (2000). Precipitation and damaging floods: Trends in the United States, 1932–97. *Journal of Climate*, *13*(20), 3625–3637. https://doi.org/10.1175/1520-0442(2000)013 < 3625:PADFTI>2.0.CO;2

Reclamation (2014). Downscaled CMIP3 and CMIP5 hydrology climate projections: Release of hydrology projections, comparison with preceding information, and summary of user needs. *US Bureau of Reclamation*. Denver, CO. Retrieved from https://gdo-dcp.ucllnl.org/downscaled_cmip_projections/techmemo/BCSD5HydrologyMemo.pdf

Seaber, P. R., Kapinos, F. P., & Knapp, G. L. (1987). *Hydrologic unit maps. U.S. Geological Survey Water-Supply Paper 2294*. Denver, CO: U.S. Geological Survey.

Smith, A. B., & Matthews, J. L. (2015). Quantifying uncertainty and variable sensitivity within the US billion-dollar weather and climate disaster cost estimates. *Natural Hazards*, *77*(3), 1829–1851. https://doi.org/10.1007/s11069-015-1678-x

Taylor, K. E., Stouffer, R. J., & Meehl, G. A. (2012). An overview of CMIP5 and the experiment design. *Bulletin of the American Meteorological Society*, *93*, 485–498. https://doi.org/10.1175/BAMS-D-11-00094.1

Trenberth, K. E. (1999). Conceptual framework for changes of extremes of the hydrological cycle with climate change. *Climatic Change*, *42*, 327–339.

Trenberth, K. E., Cheng, L., Jacobs, P., Zhang, Y., & Fasullo, J. (2018). Hurricane Harvey links to ocean heat content and climate change adaptation. *Earth's Future*, *6*(5), 730–744. https://doi.org/10.1029/2018EF000825

U.S. Army Corps of Engineers (2000). Economic Guidance Memorandum (EGM 01–03): Generic depth-damage relationships. http://planning.usace.army.mil/toolbox/library/EGMs/egm01–03.pdf

van der Wiel, K., Kapnick, S. B., van Oldenborgh, G. J., Whan, K., Philip, S., Vecchi, G. A., et al. (2017). Rapid attribution of the August 2016 flood-inducing extreme precipitation in south Louisiana to climate change. *Hydrology and Earth System Sciences*, *21*(2), 897–921. https://doi.org/10.5194/hess-21-897-2017

Ward, P. J., Jongman, B., Aerts, J. C. J. H., Bates, P. D., Botzen, W. J. W., Diaz Loaiza, A., et al. (2017). A global framework for future costs and benefits of river-flood protection in urban areas. *Nature Climate Change*, *7*(9), 642–646. https://doi.org/10.1038/nclimate3350

Willner, S. N., Otto, C., & Levermann, A. (2018). Global economic response to river floods. *Nature Climate Change*, *8*(7), 594–598. https://doi.org/10.1038/s41558-018-0173-2

Wobus, C., Gutmann, E., Jones, R., Rissing, M., Mizukami, N., Lorie, M., et al. (2017). Modeled changes in 100 year flood risk and asset damages within mapped floodplains of the contiguous United States. *Natural Hazards and Earth System Sciences Discussions*, 1–21. https://doi.org/10.5194/nhess-2017-152